SPE 75235

Near-Well Reservoir Monitoring Through Ensemble Kalman Filter

Geir Nævdal, Trond Mannseth, SPE, and Erlend H. Vefring, SPE, RF- Rogaland Research

This paper was prepared for presentation at the SPE/DOE Improved Oil Recovery Symposium held in Tulsa, Oklahoma U.S.A., 13–17 April 2002.

Abstract

In the management of reservoirs it is an important issue to utilize the available data in order to make accurate forecasts. In this paper a novel approach for frequent updating of the near-well reservoir model as new measurements becomes available is presented. The main focus of this approach is to have an updated model usable for forecasting. These forecasts should have initial values that are consistent with recent measurements.

The novel approach is based on utilizing a Kalman filter technique. The idea behind the Kalman filter is to incorporate the information from the measurements into the current estimate of the state of the model, taking into account the uncertainty that belongs both to the state of the model and the measurements. The uncertainty of the model is updated simultaneously with the model itself. A benefit of this approach compared to usual history matching is that the initial values for the forecasts will be in better agreement with the current measurements.

Originally, the Kalman filter had shortcomings for large, non-linear models. During the last decade, however, Kalman filter techniques has been further developed, and applied successfully for such models within oceanographic and hydrodynamic application. This work is based on use of the ensemble Kalman filter. The ensemble Kalman filter is easy to implement, and have some good properties for non-linear problems. Here, we demonstrate the use of this technique within near-well reservoir monitoring, focusing on its performance in forecasting the future production.

Introduction

Several different smart well systems are available with different functionality. The simplest systems consist of sliding sleeves which only can be open or shut and without any monitoring. The most advanced systems consist of infinitely variable chokes and extensive monitoring like pressure, temperature, multi-phase metering, and resistivity and seismic sensors for tracking near well fluid contacts.

The smart well systems are motivated by the possibility of improved reservoir management. Remote choking or shutting zones with poor performance will cause an immediate response on the well performance without any expensive well intervention.

Another benefit of smart well systems is improved reservoir monitoring. Smart wells systems add value by enhancing workflow cycles containing the key elements of measurement, modeling and control. Several papers[1,2,3,4] have been presented where the possible benefits of using smart well systems have been quantified. In all these papers the reservoir model is assumed to be known. However, a key element in the measurement, modeling and control loop is how to update the near well reservoir model based on the measurements. This is the focus of the present paper. A novel approach for updating a near-well reservoir model based on measurements in the well will be presented. The approach applies a Kalman filter technique and both the reservoir properties and the state of the reservoir is updated. Benefits of this approach is that the initial values of the forecasts will be in better agreement with the current measurements and that the methodology is well suited for frequent updating of the near well model.

An alternative methodology for updating the near-well reservoir model consist in finding the reservoir properties which gives the least difference between measured data and model results within a given time interval.[5]

We start by describing the reservoir model. Then the ensemble Kalman filter methodology applied to near well reservoir modeling is presented. Examples of application of the methodology are given, and finally some conclusions are drawn.

The reservoir model

The model equations for two-phase, immiscible porous-media flow with isotropic permeability are (see, e.g. Aziz & Settari[6])

$$\nabla \cdot \left(\frac{k_{ro} k}{\mu_o B_o} \left(\nabla p_o - \gamma_o \nabla z \right) \right) = \frac{\partial}{\partial t} \left(\frac{\phi S_o}{B_o} \right) + q_o \,, \quad \ldots\ldots (1)$$

$$\nabla \cdot \left(\frac{k_{rg} k}{\mu_g B_g} \left(\nabla p_g - \gamma_g \nabla z \right) \right) = \frac{\partial}{\partial t} \left(\frac{\phi S_g}{B_g} \right) + q_g \,, \quad \ldots\ldots (2)$$

$$S_o + S_g = 1 \,, \quad \ldots\ldots (3)$$

$$p_g - p_o = P(S_g) \quad \ldots\ldots (4)$$

We assume that the porosity is known all over the reservoir, while the permeability is unknown, along with the solution variables; oil pressure and gas saturation. The remaining quantities in equations (1) – (4), except the external volumetric flow rates, are known functions of the solution variables.

The external volumetric flow rates are specified to be zero at outer boundaries. A multi-segment well model[7] is applied to couple reservoir and wellbore flows.

The ensemble Kalman filter for near-well reservoir monitoring

The values of several important quantities, as for instance porosity, permeability and relative permeability, in the reservoir model varies in the reservoir, and quantities as porosity and permeability are not even accessible for measurement except from core samples. The reservoir flow depends to large extent on these quantities, and therefore the quality of the forecasts made from reservoir simulations depends on the ability to give reasonable values to these quantities. The approach suggested in this paper is to improve the forecasts by updating the relevant physical quantities, based on the measurements that become available during production, as well as using the information gained from core samples. A similar approach, to the one presented here, has been applied in the study of underbalanced drilling[8].

The Kalman filter[9] was originally developed for linear models. An early approach for treating non-linear models is the extended Kalman filter[10]. A problem with the extended Kalman filter is that the number of simulations needed at each step is at the same order as the number of state variables. For large systems this will generally be too time-consuming. The extended Kalman filter is based on linearization and has shortcomings for strongly non-linear models. Recently, progress has been made addressing both these problems, and new variants of Kalman filters have been applied within meteorology and oceanography. One of these filters, the ensemble Kalman filter[11] is very easy to implement, and we have used this for estimating our unknown model parameters.

Using the Kalman filter it is possible to combine the information obtained from the measurements with the model to get an improved estimate of the state vector of the system. Our state vector contains the values for each grid block of the time dependent variables pressure and gas saturation as well as a value for the permeability in each grid block. Such an extension of the state vector to include model parameters has been applied both in the study of underbalanced drilling[8] and in a test model used in atmospheric research[12]. In these applications the number of model parameters is in the range from 1-9, a modest number compared to the number of model parameters included in the state space in our applications.

In addition to extend the state parameters with model parameters, it is necessary to include all measurements that is connected to the state variables by a non-linear relation in the state vector, due to the formulation of the ensemble Kalman filter. This means that the state vector has to be further augmented with the measurements obtained from pressure sensors and multi-phase metering located in the well.

We will now give a short presentation of the implemented filter, and discuss some details on the actual implementation for this study. This presentation follows closely the presentation given in Lorentzen[8].

To combine the information from the measurements with the model in a proper way, we need both to know the uncertainty in the current estimate of the state and the uncertainty in the measurements. We assume that the errors in the measurements are statistically independent, and with known variances. This gives a covariance matrix Σ for the measurement errors. In the ensemble Kalman filter the covariance matrix of the estimate of the states are obtained using statistics built by an ensemble of state vectors. After the ensemble is updated by taking into account new measurements we go through the following steps.

Denote the state vector for the j'th member of the ensemble after inclusion of the measurement by $\vec{s}_j^{\,a}$. Each state vector is used as initial value to the simulator for a forward simulation that is run to the time when the next measurements are taken into account. The j'th state vector prior to the inclusion of the next measurements is

$$\vec{s}_j^{\,f} = f(\vec{s}_j^{\,a}) + \vec{\psi}_j \,, \quad \ldots\ldots (5)$$

where $f(\vec{s}_j^{\,a})$ denotes the updating of the state vector done by the simulator and $\vec{\psi}_j$ is a stochastic contribution representing the model error. The model error we use is normally distributed with zero mean and covariance matrix Ψ. More details on the specification of Ψ will be given below.

To take into account the measurements we use the covariance matrix of the ensemble around the ensemble mean. The mean value of the ensemble is given by

$$\hat{\vec{s}} = \frac{1}{n} \sum_{i=1}^{n} \vec{s}_j^{\,f} \,, \quad \ldots\ldots (6)$$

and the ensemble covariance matrix is

$$R = \frac{1}{n} \sum_{i=1}^{n} \sum_{j=1}^{n} (\vec{s}_j^{\,f} - \hat{\vec{s}})(\vec{s}_i^{\,f} - \hat{\vec{s}})^T \,, \quad \ldots\ldots (7)$$

where n is the number of members in the ensemble. For proper use of the filter an ensemble of observations is needed[13]. This is defined by

$$\vec{d}_j = \vec{d} + \vec{\varepsilon}_j \,, \quad \ldots\ldots (8)$$

where $\vec{d}$ is the actual observation and ε_j is drawn from a normal distribution with zero mean and covariance matrix Σ.

The observation vector $\vec{d}$ is related to the state vector $\vec{s}$ through the equation $\vec{d} = H\vec{s}$, for an appropriate matrix H. The state vectors in the ensemble are updated using the gain matrix

$$G = RH^T(HRH^T + \Sigma)^{-1}, \quad \text{.....(9)}$$

through the equation

$$\vec{s}_j^{\,a} = \vec{s}_j^{\,f} + G(\vec{d}_j - H\vec{s}_j^{\,f}) \quad \text{.....(10)}$$

A major issue with the ensemble Kalman filter is the size of the ensemble. The optimal size of the ensemble for our application is a subject for further research. Experience in the oceanographic science[14] has indicated that the filter may function using a size of the ensemble in the range 100 – 500. We have chosen to use 100 members in the ensemble. This means that 100 forward simulations are needed. With increasing computational power, the challenge faced because of the size of the ensemble may be reduced, and it should be remarked that the ensemble Kalman filter is well suited for parallelization. A modification of the ensemble that reduces the computational burden has been proposed[15], and it will be investigated in further work if this modification is suitable for the present problem.

In the specification of the covariance matrix for the modeling error, Ψ, we make the assumption that the dominating term is the uncertainty in the permeability. The covariance matrix for the model error is block-diagonal, with two blocks. The first block consists of the model error in the logarithm of the permeability. This is modeled using a distance dependent correlation function, such that the permeability in grid blocks that are located close to each other are updated in a correlated manner, whereas there is small correlation in the updating of the permeability between grid blocks that are located far apart. Our assumptions is that the major features of the model uncertainty is taken into account by the model uncertainty in the permeability, and therefore we only use a very small, and uncorrelated, model error for the states representing the pressure and saturation of the grid blocks as well as for the state variables that are included to take into account the nonlinear well measurements.

It is our experience that proper specification of the covariance matrix for the modeling error is crucial to get good performance of the filter. Obtaining guidelines for this specification will be an important topic for further research.

In the examples we present, all measurements are generated synthetically by running the model with a given permeability, and adding noise to the obtained values to generate measurements. As covariance matrix, Σ, for the measurement error we have used the same covariance matrix as used when generating the measurements. In a field implementation, the covariance matrix for the measurement errors Σ should take into account the uncertainty in the measurement devices, but also include uncertainty in the positioning of the measurement gauges, and inaccuracies due to the applied numerical method[16].

Examples

Common setup of the examples. In the examples we present, we have kept the same reservoir and well configuration. The scenario is one horizontal producer, an immiscible two-phase system with oil and gas. The PVT properties and relative permeability curves are adapted from[17], and kept fixed both while generating data and while running the ensemble Kalman filter. The reservoir grid has dimension $16 \times 1 \times 16$, where the last coordinate refers to the vertical direction. The dimension of each grid block is $30 \times 100 \times 30$ ft. We have used a constant porosity in the reservoir, except for the top layer which is used to emulate a gas cap. The porosity of the grid blocks in the top layer is set to 1000, for all other grid blocks the porosity is 0.3. The depth of the top layer is 6970 ft.

The well has its heel in grid block (4,1,14), and it is perforated in three grid blocks, (5,1,14), (9,1,14) and (13,1,14) (see Figure 1). The depth of the well is 7375 ft, corresponding to the middle of grid block 14 in the vertical direction (where the vertical direction is numbered from the top). In the perforated blocks, the annulus section is connected to the production tubing of the well through chokes.

While using the filter we assume that the following quantities are available: Estimate of the permeability of the grid blocks penetrated by the well (from core samples), in addition to measurements during production. The quantities measured during productions are the bottom-hole pressure and pressure in the three annulus sections of the well, the total production of oil and gas, and the inflow of these two phases through each annulus section.

The uncertainties in the different measurements are shown in Table 1.

Table 1: Measurement uncertainties.

Quantity	Uncertainty (1 std. deviation)
Permeability of grid block	3 %
Pressure	4 psia
Oil saturation	10 %
Gas saturation	10 %

Production data are sampled at every 0.1 days the first day, thereafter once every day. The known permeability values are taken into account every time the state vector is updated.

The permeability used in the examples is shown in Figure 1. The well is shown in red (perforated zones) and white. The heel of the well is located to the left. The well is set to produce at an oil rate of 1500 bbl/day, but with a limitation on the gas production on 10000 Mscf/day.

The difference between the two examples is in the choke settings. In Example the opening of the choke in zone 3 is one half of the opening used in zone 1 and 2. In example 3 the opening of the chokes is the same for all three zones. In Example 1 the limitation on gas production is met after 83 days, in Example 2 after 96 days.

In this setting, the focus has only been on the ability to produce reliable forecast for the inflow, but combining

the technique for producing forecasts with steering is a challenging problem.

Result from Example 1. Figures 2-8 show the true solution, the measurements and the estimated solution for different measured quantities.

Figure 2 shows the bottom-hole pressure. The uncertainties in the pressure measurements are low, and there is no visible difference between the estimated pressure and the true pressure. The same holds for the pressure measurements in each of the annulus sections.

Figures 3 – 5 show the production of oil for the three inflow zones. One can observe that the estimated rates follow the true curves quite closely, although the measurements are noisy. A similar observation can be done for the gas inflows, see Figure 6 – 8, although the estimate are fluctuating more when the inflow is increasing. For the total production of oil and gas the filter and the true curve coincides, so the plots are omitted.

We evaluate the performance of the ensemble Kalman filter by considering the quality of the forecasts of production. Figures 9 – 14 show forecasts of the oil and gas inflow to each of the three inflow zones. The first forecast is done after 0.1 days, which is the first measurement of the production data. At this point the forecast of the gas inflow is misleading, it is predicted that the highest gas inflow will be in Zone 3, not in Zone 1. While more production data becomes available, this error in the forecasts is gradually removed.

The next forecast is shown after 26 days. This is before there is any significant gas inflow to the well. The quality of the forecasts in zone 1 and zone 3 are significantly improved compared to the forecasts after 0.1 days.

The last forecast is shown after 73 days. There has been some further improvement in the forecast of the future gas production from each of the zones.

Result from Example 2. Figures 15 - 20 show the true solution, the synthetic measurements, and the estimated solution for the oil and gas inflow to the three zones in Example 2.

Figures 15 – 17 show the production of oil for the three inflow zones. One can observe that the estimated rates follow the true curves quite closely, although the measurements are noisy. It seems that the filter works some what better for the zones with higher inflow rates.

Figures 18 – 20 show the production of gas for the three inflow zones. There is very low difference between the estimated value and true value when the gas inflow is low. As the inflow increases, the estimated curve has larger fluctuations about the true curve. There are two factors that both are reasonable explanations for this behavior. One of the factors is that the measurement noise is relative, and therefore larger for larger inflows. In addition the system is run from an equilibrium state, leading to an increased uncertainty about the gas saturation in the reservoir with time.

Figure 21 – 26 show forecasts of the oil and gas inflow to the three zones. The forecasts are shown after 0.1, 16 and 64 days. Although the limitation on total production of gas is met later in this example than the previous one, there is significant gas inflow earlier in zone 3 for this example. The performance of the forecasts of gas production after 64 days is much better than after only 0.1 days.

There are indications that the early measurements are more important for improving the forecast than later measurements, and the forecast of the gas production seems to be more influenced by the updating than the oil production in these two examples.

To study the effect of the measurements at different time intervals, and the possibilities for tuning different variables in the filter is a topic for further research.

Conclusions

A new methodology using the ensemble Kalman filter technique for forecasting production of a near-well reservoir has been presented. The technique has been studied through synthetic examples. With this technique, one is able to track the production of the two phases in each of the three inflow zones with much better accuracy than if these values are obtained solely from the measurements of the same quantities. Even more important is it that the reservoir model is updated, such that forecasts can be computed which are consistent with the recent measurements. This could be further exploited in control of smart wells. It is seen that, generally, the forecasts are improved while more measurements becomes available.

Nomenclature

B = Formation volume factor
d = Measurement
G = Kalman gain
H = Measurement matrix
k = Permeability
k_r = Relative permeability
n = Number of members in ensemble
P = Capillary pressure
p = Pressure
q = External volumetric flow
R = Ensemble error covariance matrix
S = Saturation
$\vec{S}$ = Member of ensemble
t = Time
z = Spatial vertical coordinate
γ = Product of mass density and acceleration of gravity
μ = Viscosity
Σ = Measurement error covariance matrix
ε = Measurement error
Ψ = Model error covariance matrix
ψ = Model error
Φ = Porosity

Subscripts

g = Gas
j = Related to the ensemble
o = Oil

Superscripts

a = *Analyzed.*
f = *Forecast.*

Acknowledgements

This work has been supported financially by the Norwegian Research Council.

References

1. Jalai, Y., Bussear, T. and Sharma, S., "Intelligent Completion Systems – The Reservoir Rationale", paper SPE 50587 presented at the 1998 SPE EuropeanPetroleum Conference held in the Hague,The Netherlands, 20 –22 October 1998.'
2. Sinha, S., Kumar, R.,Vega, L. and Jalai, Y., "Flow Equilibration Towards Horizontal Wells Using Downhole Valves", paper SPE68635 presented at the SPE Asia Pacific Oil and Gas Conference and Exhibition held in Jakarta, Indonesia, 17-19 April 2001.
3. Yeten, B. and Jalali Y., "Effectiveness of Intelligent Completions in a Multiwell Development Context", paper SPE 68077 presented at the 2001 SPE Middle East Oil Show held in Bahrain, 17-20 March 2001.
4. Yu, S. and Davies, D. R., "The Modelling of Advanced "Intelligent" Well – An Application", paper SPE 62950 presented at the 2000 SPE Annual Technical Conference and Exhibition, Dallas, Texas, 1 – 4 October 2000.
5. Mannseth, T., Nordtvedt, J. E., and Nævdal, G.: "Optimal Management of Advanced Wells through Fast Updates of the Near-Well Reservoir Model", Proceedings of the 7th European Conference on the Mathematics of Oil Recovery, Baveno, Italy, 5 – 8 Spetember, 2000.
6. Aziz, K. and Settarri, A.: *Petroleum Reservoir Simulation*. Applied Science, London, (1979).
7. Eclipse Technical Description. 2000A. Schlumberger. (2000).
8. Lorentzen, R.J., Fjelde, K.K., Frøyen, J., Lage, A.C.V.M., Nævdal, G., and Vefring, E.H.: "Uncerbalanced and Low-head Drilling Operations: Real Time Interpretation of Measured Data and Operational Support." Paper SPE 71384 presented at the 2001 SPE Annual Technical Conference and Exhibition held in New Orleans, Lousiana, 30 September – 3 October (2001).
9. Grewal, M.S. and Andrews, A.P.: *Kalman Filtering:Theory and Practice*. Prentice Hall, Englewood Cliffs, New Jersey (1983).
10. Maybeck, P.S.: *Stochastic Models, Estimation, and Control*. Vol. 2. Academic Press, New York (1982).
11. Evensen, G.: "Sequential Data Assimilation with Nonlinear Quasi-geostrophic Model using Monte Carlo Methods to forecast Error Statistics." *J. Geophys. Res*. Vol. 99 (C5), pp. 10 143 – 10 162, (1994).
12. Anderson, J. L.: "An Ensemble Adjustment Kalman Filter for Data Assimilation." *Monthly Weather Review*. Vol. 129, pp. 2884 – 2903, (2001).
13. Burgers, G., van Leeuvwen, P. J., and Evensen, G.: "Analysis Scheme in the Ensemble Kalman Filter." *Monthly Weather Review*. Vol. 126, pp. 1719 – 1724, (1998).
14. Evensen, G.: "Application of Ensemble Integrations for Predictability Studies and Data Assimilation." Published in: *Monte Carlo Simulations in Oceanography*, Proceedings 'Aha Huliko'a Hawaiian Winter Workshop, University of Hawaii at Manoa, January 14--17, (1997).
15. Heemink, A.W., and Verlaan, M., and Seegers, A.J.: "Variance reduced Ensemble Kalman Filtering." *Monthly Weather Review*. Vol. 129, pp. 1718 – 1728, (2001).
16. Cohn, S.E.: "An Introduction to Estimation Theory." *Journal of the Meteorological Society of Japan*. Vol. 75, pp. 257 - 288, (1997).
17. Eclipse Reference Manual 2000A. Schlumberger (2000).

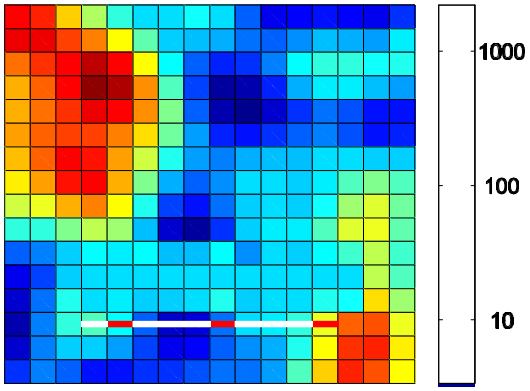

Figure 1. The true permeability. The well is shown in red and white. The perforated part of the well is red. The permeability is given in mD.

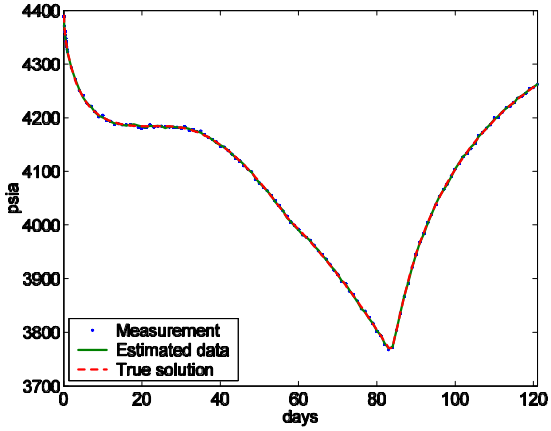

Figure 2. Bottom hole pressure in Example 1.

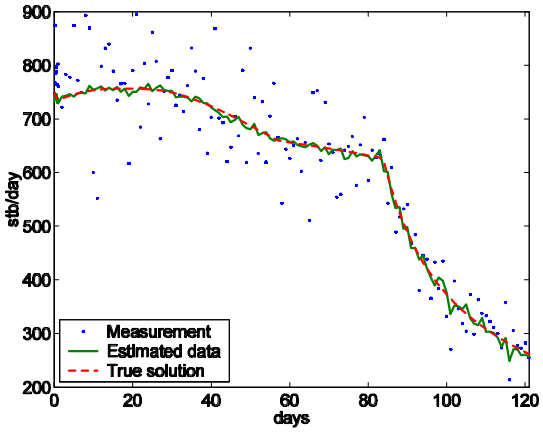

Figure 3. Oil inflow in zone 1 (grid block (5,14), heel of well) in Example 1.

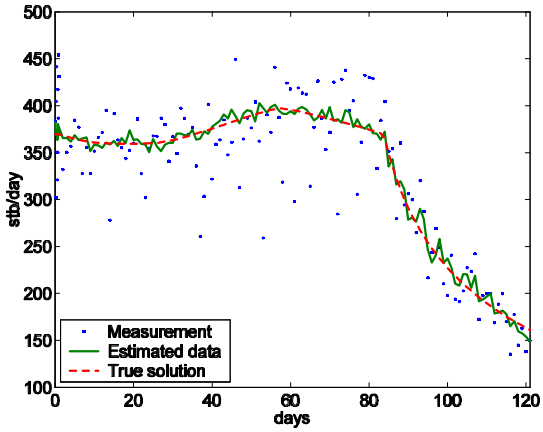

Figure 4. Oil inflow in zone 2 (grid block (9,14)) in Example 1.

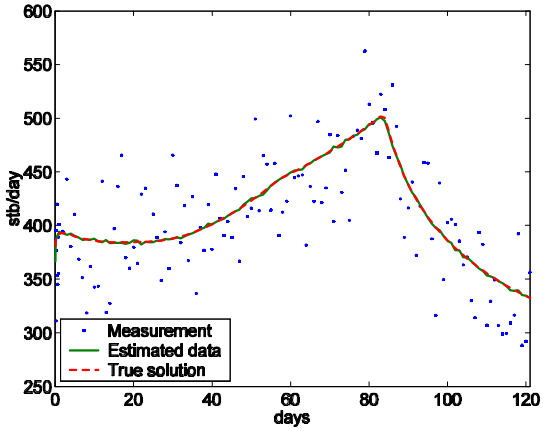

Figure 5. Oil inflow in zone 3 (grid block (13,14), toe of well) in Example 1.

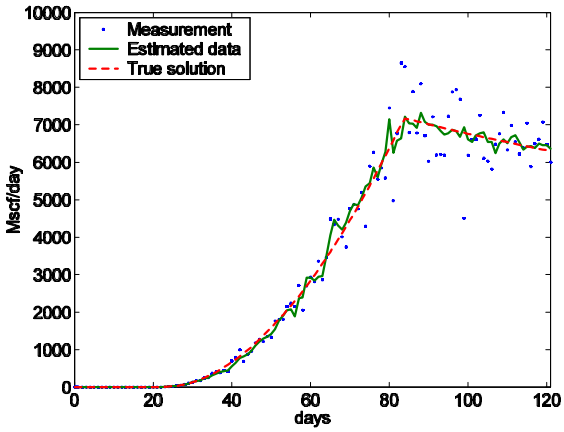

Figure 6. Gas inflow in zone 1 in Example 1.

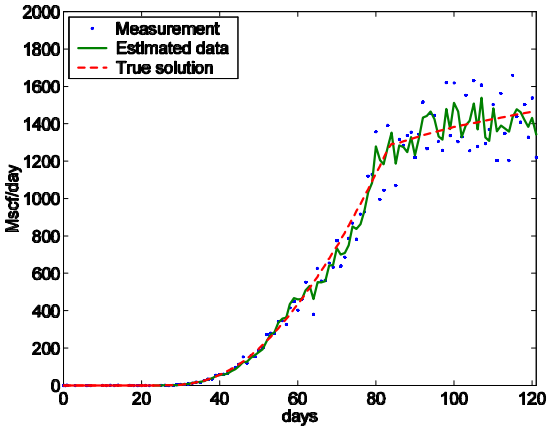

Figure 7. Gas inflow in zone 2 in Example 1.

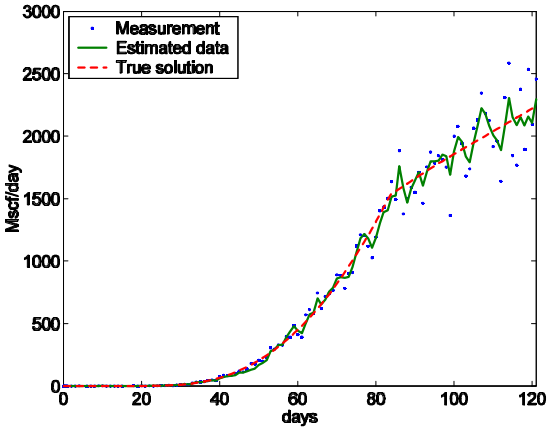

Figure 8. Gas inflow in zone 3 in Example 1.

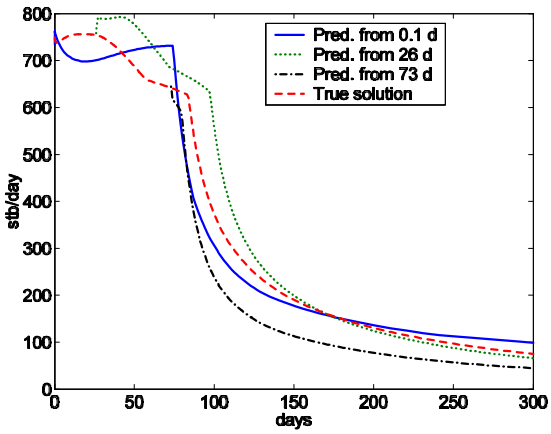

Figure 9. Forecast of oil inflow in zone 1 in Example 1.

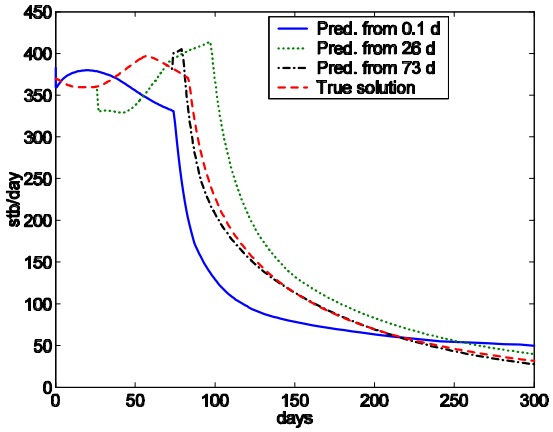

Figure 10. Forecast of oil inflow in zone 2 in Example 1.

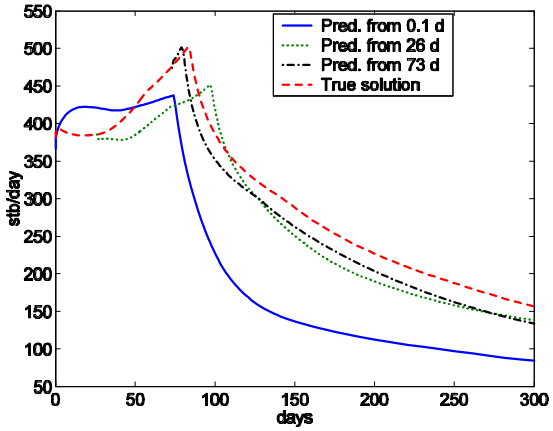

Figure 11. Forecast of oil inflow in zone 3 in Example 1.

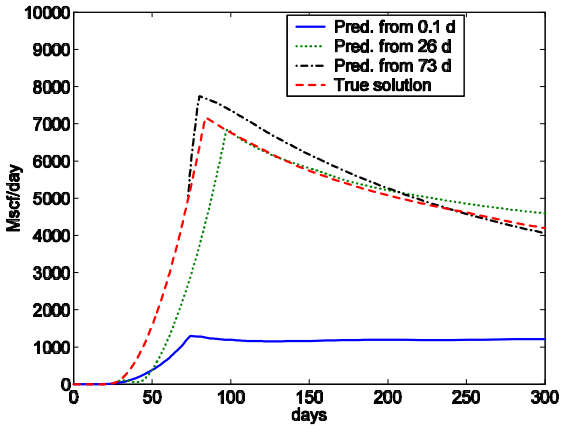

Figure 12. Forecast of gas inflow in zone 1 in Example 1.

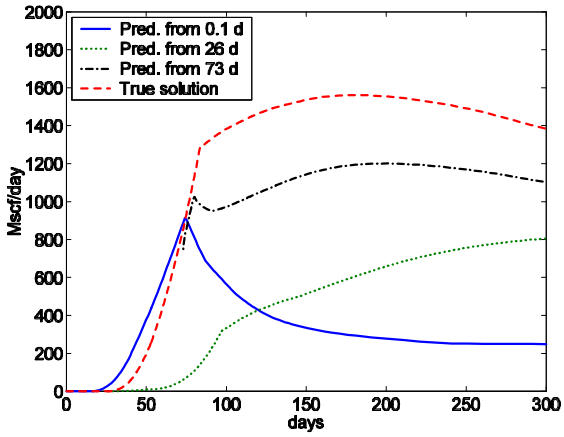

Figure 13. Forecast of gas inflow in zone 2 in Example 1.

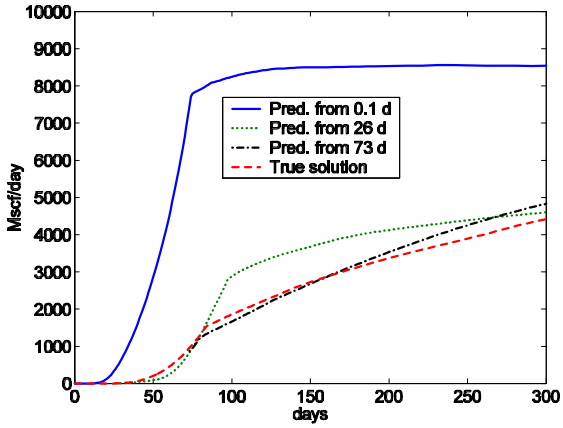

Figure 14. Forecast of gas inflow in zone 3 in Example 1.

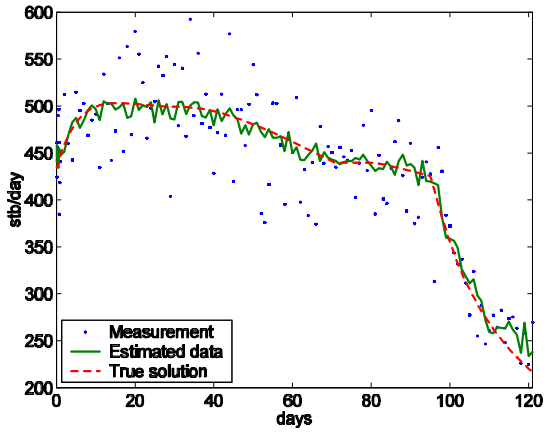

Figure 15. Oil inflow in zone 1 in Example 2.

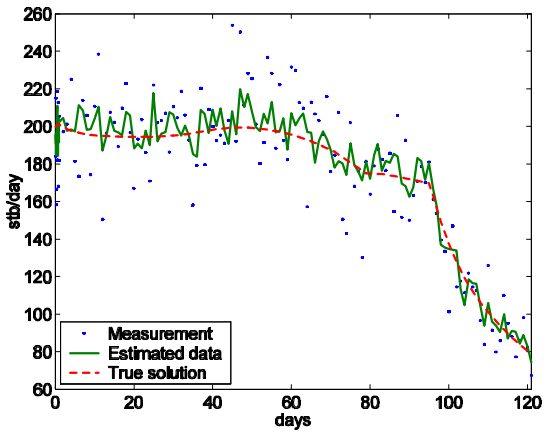

Figure 16. Oil inflow in zone 2 in Example 2.

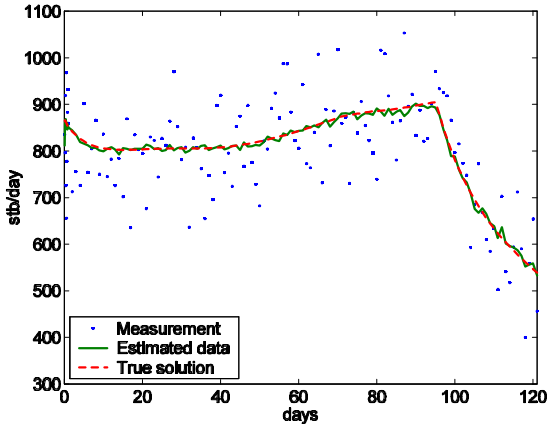

Figure 17. Oil inflow in zone 3 in Example 2.

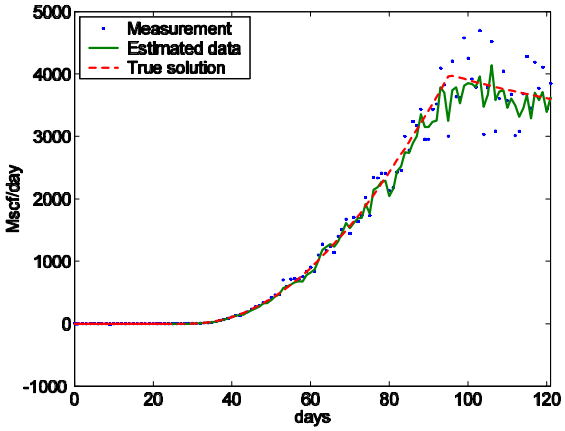

Figure 18. Gas inflow in zone 1 in Example 2.

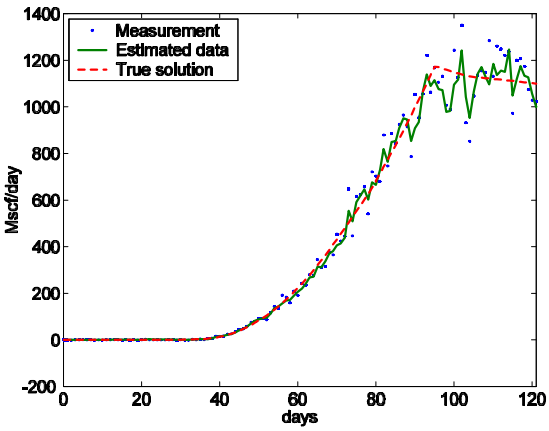

Figure 19. Gas inflow in zone 2 in Example 2.

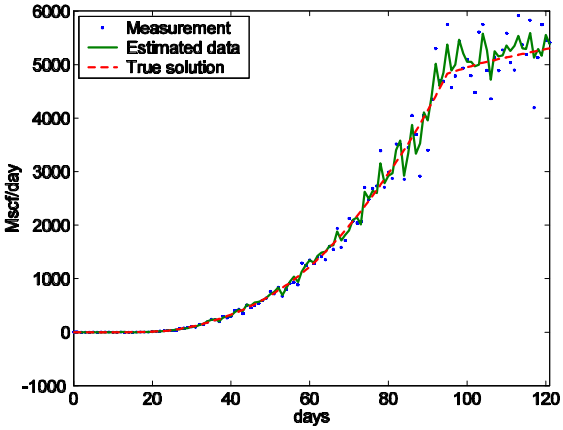

Figure 20. Gas inflow in zone 3 in Example 2.

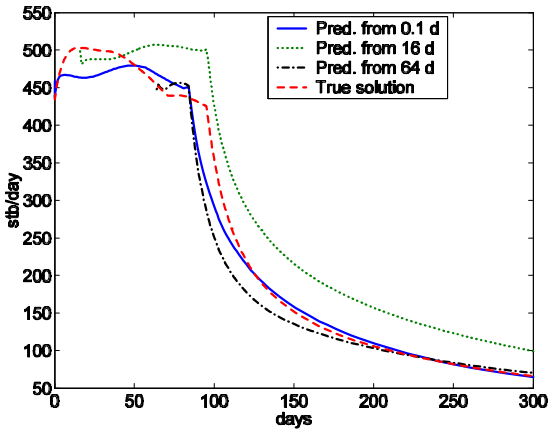

Figure 21. Forecast of oil inflow in zone 1 in Example 2.

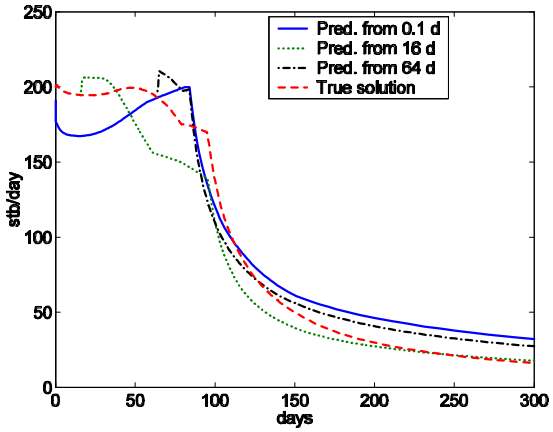

Figure 22. Forecast of oil inflow in zone 2 in Example 2.

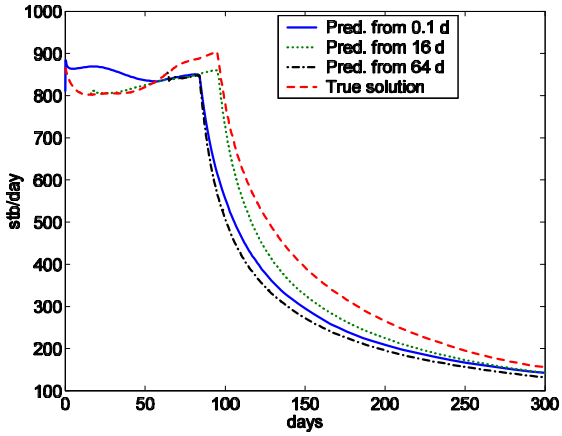

Figure 23. Forecast of oil inflow in zone 3 in Example 2.

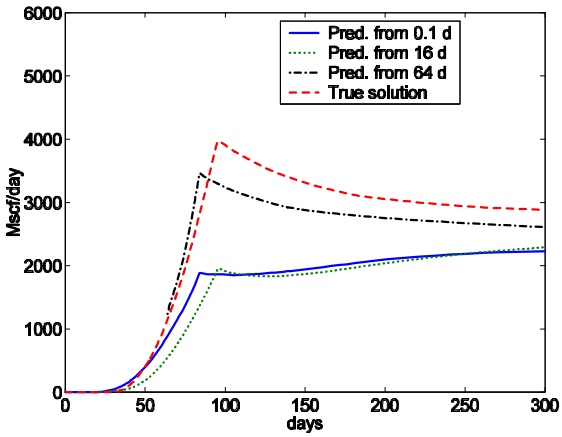

Figure 24. Forecast of gas inflow in zone 1 in Example 2.

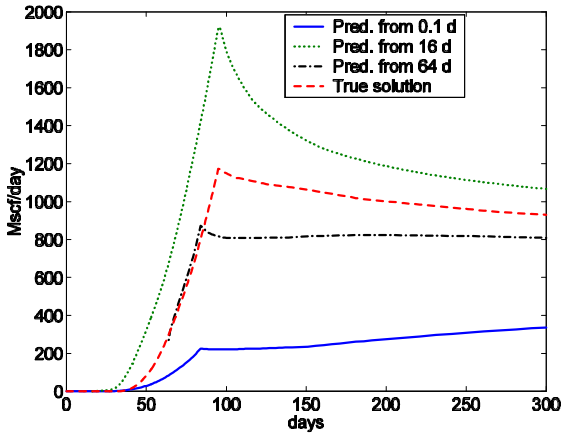

Figure 25. Forecast of gas inflow in zone 2 in Example 2.

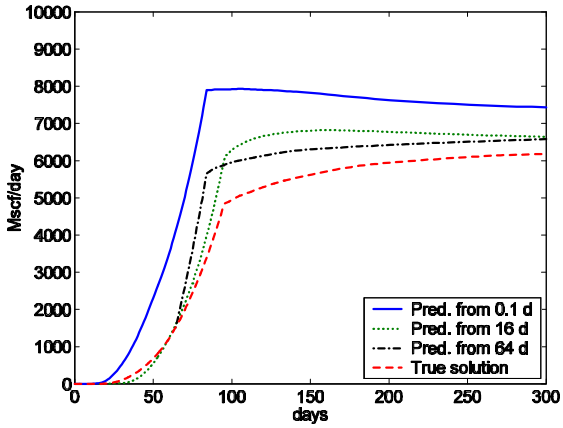

Figure 26. Forecast of gas inflow in zone 3 in Example 2.